

Supplementary Material

A Novel Artificial Hemoglobin Carrier Based on Heulandite-Calcium Mesoporous Aluminosilicate Particles

Dino Jordanoski ¹, Damjana Drobne ¹, Neža Repar ¹, Iztok Dogša ¹, Polona Mrak ¹, Romana Cerc-Korošec ², Andrijana Sever Škapin ³, Peter Nadrah ³, Nataša Poklar Ulrih ^{1*}

¹ University of Ljubljana, Biotechnical Faculty, Jamnikarjeva 101, 1000 Ljubljana, Slovenia; Dino Jordanoski: dj6841@student.uni-lj.si. Damjana Drobne: damjana.drobne@bf.uni-lj.si. Neža Repar: neza.repar@bf.uni-lj.si. Iztok Dogša: iztok.dogsa@bf.uni-lj.si. Polona Mrak: polona.mrak@bf.uni-lj.si. Nataša Poklar Ulrih: natasa.poklar@bf.uni-lj.si.

² University of Ljubljana, Faculty of Chemistry and Chemical Technology, Večna pot, 1000 Ljubljana, Slovenia; Romana Cerc-Korošec: romana.cerc-korosec@fkkt.uni-lj.si.

³ Slovenian National Building and Civil Engineering institute, Dimičeva ulica 12, 1000 Ljubljana, Slovenia; Andrijana Sever Škapin: andrijana.skapin@zag.si. Peter Nadrah: peter.nadrah@zag.si.

* Correspondence: Nataša Poklar Ulrih: natasa.poklar@bf.uni-lj.si; Tel.: (+386 1 3203 780, 100 Ljubljana, Slovenia)

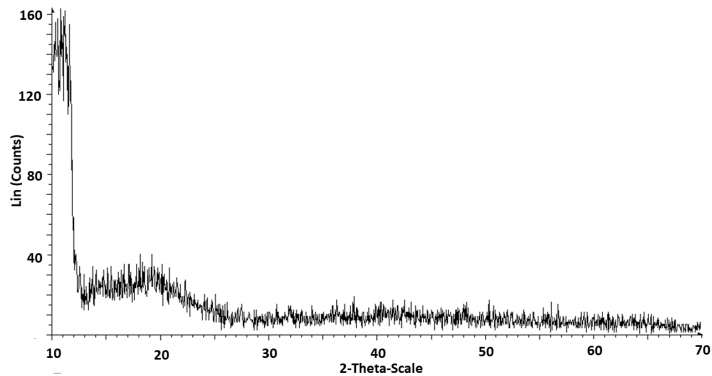
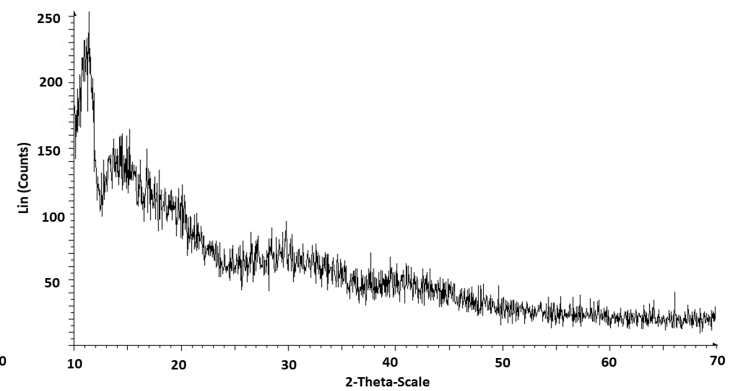
A**B**

Figure S1. X-ray diffraction patterns of empty liposomes (LB) (**A**) and liposome-encapsulated MSPs (LB-MSPs) (**B**).

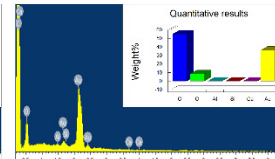
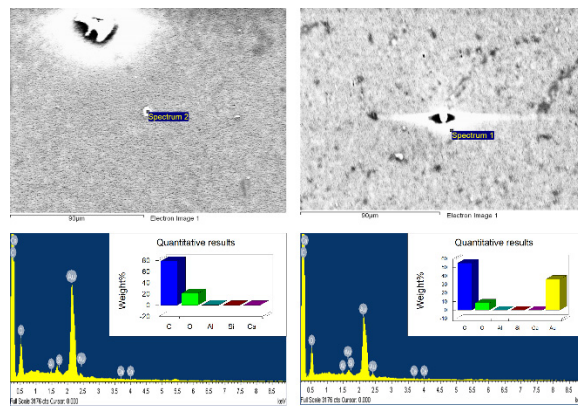
A

Figure S2. Field emission SEM energy dispersive spectroscopy analysis of empty liposomes (**A**) and liposome-encapsulated MSPs (**B**).

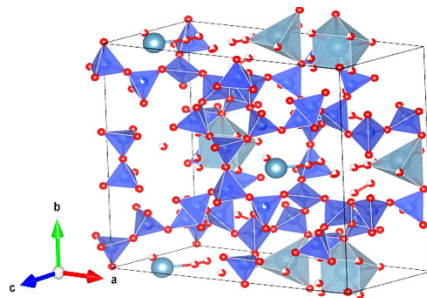


Figure S3. Crystal structure of heulandite-Ca, visualized using the VESTA software, with atom coordinates from the American Mineralogist Crystal Structure Database (VESTA, n.d.).

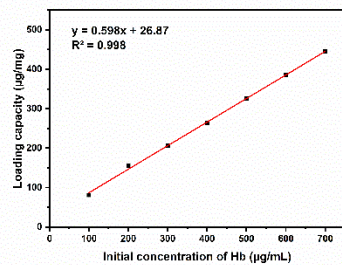


Figure S4. Hemoglobin-loading capacity for MSPs at low-loading concentrations, using a plate reader (Safire 2; Tecan; absorbance, 405 nm; 400-700 µg/mL).

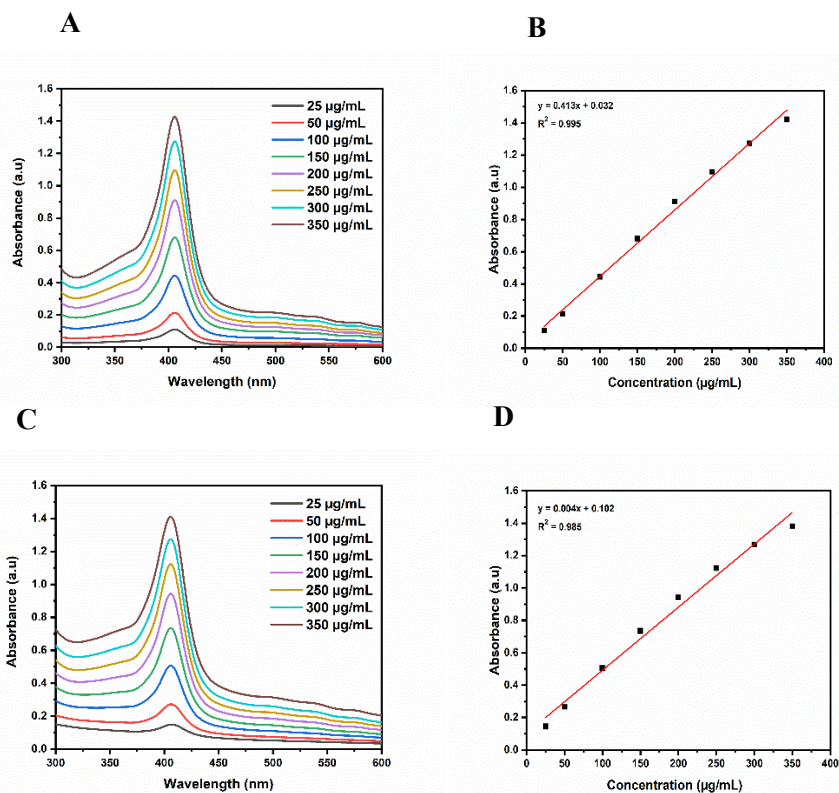


Figure S5. (A, C) UV-VIS absorbance spectra of Hb (25-350 µg/mL; 1 mM PB as control) (A) and Hb-loaded MSPs (25-350 µg/mL; 250 µg/mL MSPs in 1 mM PB as

control) (**C**). (**B, D**) Standard curves for absorbance (405 nm) of Hb (**B**) and Hb-loaded MSPs (**D**).

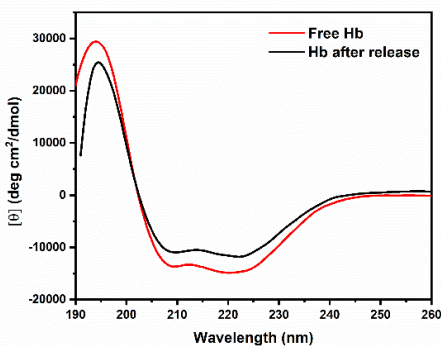


Figure S6. Far-UV circular dichroism spectra of free Hb and Hb after release from Hb-loaded MSPs.

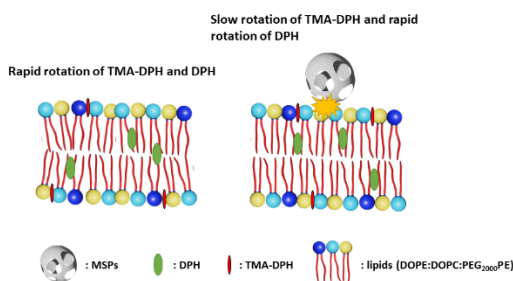


Figure S7. Schematic illustration of the MSP–liposome membrane interactions. DPH, 1,6-diphenylhexatriene; TMA-DPH, DPH trimethylammonium derivative; DOPE, 1,2-dioleoyl-*sn*-glycero-3-phosphoethanolamine; DOPC, 1,2-dioleoyl-*sn*-glycero-3-phosphocholine; PEG, polyethylene glycol.

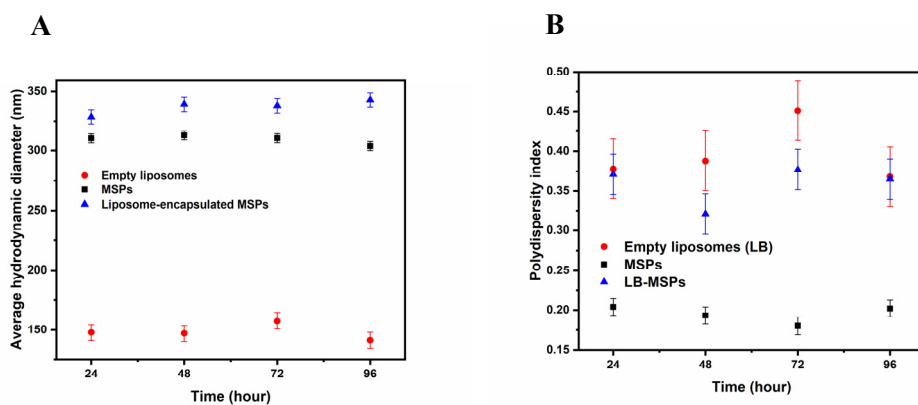


Fig. S8. (A) Size stability of LB, MSPs and LB-MSPs); (B) Corresponding PDI values.

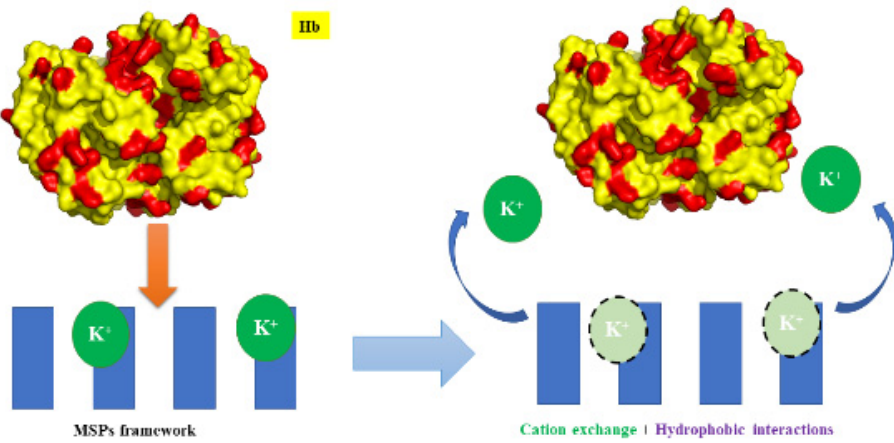


Figure S9. Schematic diagram of adsorption of hemoglobin (Protein) onto natural zeolite (heulandite-Ca). The hydrophobic surface of hemoglobin was modeled with the PyMOL software, version 2.4.1. Yellow, Hb backbone; red, Hb positively charged amino acids (i.e., Arg, His, Lys).

Table S1. Summary of hemoglobin effects upon interaction with tetraethyl orthosilicate (TEOS)-based particles and heulandite-Ca MSPs.

| Analysis technique | Particle type | |
|---|---|--|
| | TEOS-based particles | Heulandite-Ca MSPs |
| Fourier transform infrared spectroscopy | Structural changes induced | Partial denaturation and successful binding |
| Fluorescence spectroscopy | Degradation induced | Partial denaturation and successful binding |
| Circular dichroism | Displacement and denaturation | Partial denaturation |
| UV-Vis spectroscopy | Iron release induced at low particle concentrations | Iron release induced at high particle concentrations ($\geq 100 \mu\text{g/mL}$) |
| Peroxidase-like activity | Preserved redox activity of bound hemoglobin | Higher redox activity of bound hemoglobin |

| | | |
|---------------------|---|---|
| Cytotoxicity | Cytotoxic at low concentrations ($\geq 10 \mu\text{g/mL}$) | No cytotoxicity up to $\geq 100 \mu\text{g/mL}$ |
|---------------------|---|---|